Int J Adv Manuf Technol (2007) 34: 295–299
DOI 10.1007/s00170-006-0609-0

ORIGINAL ARTICLE

S. Keith Hargrove · Duowen Ding

# Determining cutting parameters in wire EDM based on workpiece surface temperature distribution

Received: 29 September 2005 / Accepted: 4 April 2006 / Published online: 23 May 2006


**Abstract** The material removal process in wire electrical discharge machining (WEDM) may result in work-piece surface damage due to the material thermal properties and the cutting parameters such as varying on-time pulses, open circuit voltage, machine cutting speed, and dielectric fluid pressure. A finite element method (FEM) program was developed to model temperature distribution in the work-piece under the conditions of different cutting parameters. The thermal parameters of low carbon steel (AISI4340) were selected to conduct this simulation. The thickness of the temperature affected layers for different cutting parameters was computed based on a critical temperature value. Through minimizing the thickness of the temperature affected layers and satisfying a certain cutting speed, a set of the cutting process parameters were determined for workpiece manufacture. On the other hand, the experimental investigation of the effects of cutting parameters on the thickness of the AISI4340 workpiece surface layers in WEDM was used to validate the simulation results. This study is helpful for developing advanced control strategies to enhance the complex contouring capabilities and machining rate while avoiding harmful surface damage.

**Keywords** WEDM · Thermal damage · FEM · Temperature distribution · Cutting parameters

## 1 Introduction

Wire electrical discharge machining (WEDM) is the most widely recognized and nontraditional machining process used in industry today. It is a thermal erosion process whereby material is removed from an electrically conductive material immersed in a liquid dielectric with a series of randomly distributed discrete electric sparks or discharges between the tool electrode and the workpiece [1]. WEDM has been replacing drilling, milling, grinding and other traditional machining operations throughout the world [2]. The recast layer, microcracking, and other damage to the workpiece material surface are the main concerns for most manufacturing applications. In the WEDM, one of the main causes of surface degradation is thermal damage due to the heat of the spark. Surface layers of the workpiece as a result of WEDM machining are the recast layer, the white layer, and the heat affected zone as shown in Fig. 1.

The recast contains a layer of unexpelled molten material. The recast layer is formed because some of the molten metal has not been expelled. The melted then recasted layer is about 1–30 μm thick. The white layer refers to hard layers of material, because of their greater resistance to etching in comparison to the bulk material. The white layer appears featureless under optical microscopes. It is known that a white layer usually consists of two layers: a white layer and a dark layer, with the bulk material beneath. The white layer is harder than either the dark layer or the bulk material. The white layer is basically a rehardened structure due to phase transformation induced by rapid heating-cooling [3]. The heat affected zone is the portion of the base metal that was not melted during brazing, cutting or welding, but whose microstructure and mechanical properties were affected. Thus, the thickness of the thermal damage surface layer including the above three zones depends on the surface temperature distribution which can be computed by the thermal properties of the workpiece material and cutting parameters. In some critical applications, for example, in the aerospace industry, the temperature increase to just below 500°C (723°K) may be a reason to reject such a part [4]. Standard wire EDM and conventional finishing EDM result in a surface layer 2–20 μm thick and rough and quick conventional EDM results in 20–200 μm surface layers [5]. In order to determine thermal damage thickness, it is important to predict machined surface temperature distribution. Blok [6] and Jaeger [7] studied

S. K. Hargrove · D. Ding (✉)
Clarence Mitchell, Jr. School of Engineering,
Morgan State University,
1700 East Cold Spring Lane,
Baltimore, MD 21251, USA
e-mail: dding@eng.morgan.edu
Tel.: +1-443-8854748

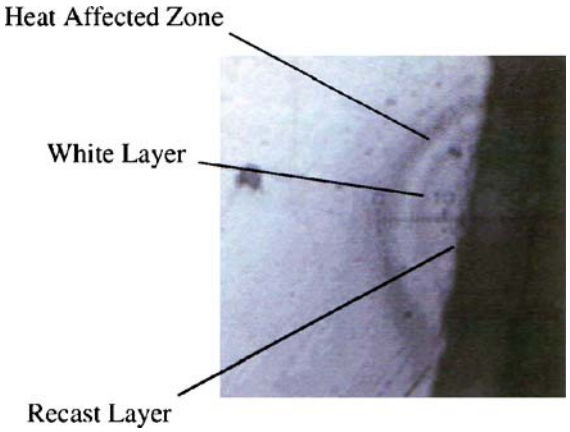


**Fig. 1** Surface layers of thermal damage in WEDM machining

the moving heat source problems that formed the basis of the analytical investigations of the temperatures rises in machining. Hahn [8] introduced the first analytical model for metal cutting temperatures. The heat transfer model in WEDM cutting has been intensively studied by Erden [9] and DiBitonto et al. [10]. Scott et al. [11] examined surface profiles by using a stochastic modeling methodology. Transient temperature distribution in the workpiece during conventional surface grinding has been studied by using numerical methods by Biermann et al. [12] and Bhattacharya et al. [13]. The micro-cracks, decrease in strength and fatigue life and possibly catastrophic failure of the workpiece can be induced by thermal stresses due to the high temperature gradients generated at the gap during WEDM machining. The temperature field and thermal stresses can be computed by finite element method (FEM) [14]. The transient temperature distribution, liquid- and solid-state material transformation, and residual stresses that are induced in the workpiece as a result of a single-pulse discharge can be predicted by FEM [15].

In this paper, the effect of the cutting parameters on the surface temperature distribution in EDM cutting is modeled by FEM. In order to minimize the damage effect of the temperature on the surface and satisfying a certain machine rate, the cutting parameters can be determined through employing an optimization model.

## 2 FEM simulation of EDM

An opportunity to assess work-piece surface damage via simulation can help determine the cutting parameters in WEDM. Thus, a simulation model that evaluates and analyses machined surface temperature may help optimize these cutting parameters. The finite element method is a numerical method which can be used for the accurate solution of complex engineering problems. The basic idea in the finite element technique is to find the solution of a complicated problem by replacing it by a simpler one. In the finite element method, the solution region is considered as built up of many small, interconnected sub-regions called finite elements. The finite element method is widely used in structural analysis, heat conduction, geo-mechanics, hydraulic and water resources engineering, and nuclear engineering. The finite element method has obvious advantages to study physically nonlinear problems, complex boundary conditions, and irregular shapes. In WEDM, because the boundary conditions are complex and the temperature field is transient, the analytical solution is hard to find. By means of the finite element method, a numerical thermal model has been developed to study machining temperatures in wire EDM. Thermal damage at the machined surface is one of the main causes of surface degradation [16]. In a cylindrical coordinate system, the differential equation for heat conduction in three-dimensional bodies is governed as follows:

$$\frac{1}{\alpha}\frac{\partial T}{\partial t}=\frac{\partial^2 T}{\partial r^2}+\frac{1}{r}\frac{\partial T}{\partial r}+\frac{1}{r^2}\frac{\partial^2 T}{\partial \varphi^2}+\frac{\partial^2 T}{\partial^2 z} \tag{1}$$

where the constant $\alpha$ ($=k/\rho c$) is the thermal diffusivity; $k$ is thermal conductivity of the workpiece; $\rho$ is density of the workpiece; $c$ is specific heat of the workpiece; $T$ is temperature of the workpiece; $r$, $z$, and $\varphi$ are coordinate axes; and $t$ is time. Heating of a workpiece due to single spark is assumed to be axisymmetric, that is, $\frac{\partial T}{\partial \varphi}=0$ , thus Eq. 1 becomes

$$\frac{1}{\alpha}\frac{\partial T}{\alpha t}=\frac{\partial^2 T}{\partial r^2}+\frac{1}{r}\frac{\partial T}{\partial r}+\frac{\partial^2 T}{\partial z^2} \tag{2}$$

A small cylindrical portion of the workpiece around a spark is separated as the domain. The heat flux and the convection heat transfer occur from the top side $\Gamma_1$ of the domain (Fig. 2).

The convection heat transfer is used to simulate heat loss to the coolant on the surface. The heat flux is used to simulate spark energy to transfer into the surface of the workpiece. Further, the boundaries $\Gamma_2$, $\Gamma_3$ and $\Gamma_4$ are at such a large distance such that there is no heat transfer

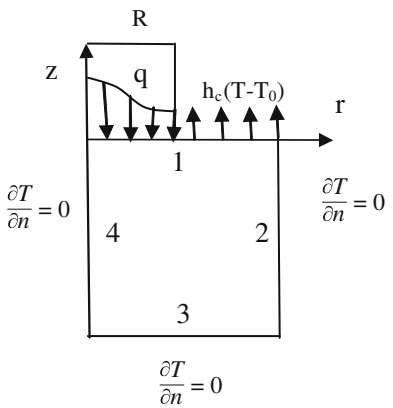


**Fig. 2** Thermal model of EDM

**Table 1** Material thermal parameters

| $k$ (Watts/mm-°K) | $H$ (Watts/mm$^2$-°K) | $\rho$ (g/mm$^3$) | $C$ (J/g K) |
|---|---|---|---|
| 0.043 | 0.01 | 0.0078 | 0.46 |

across them. Based on the above statement, the boundary condition can be expressed as follows:

$$k\frac{\partial T}{\partial z} = \begin{cases} h(T - T_0) & \text{if r} > \text{R on } \Gamma_1 \\ \text{q} & \text{if r} \le \text{R on } \Gamma_1 \\ 0 & \text{for off} - \text{time on } \Gamma_1 \end{cases} \quad (3)$$

$$\frac{\partial T}{\partial n} = 0 \quad on\ \Gamma_2, \Gamma_3\ and\ \Gamma_4$$

where $h$ is the heat transfer coefficient; $T_0$ (298°K) is the temperature of the surrounding workpiece; $q$ is the discharge energy partition fraction; and $n$ is normal to the surface.

The initial temperature $T_i$ can be taken as normal room temperature of the dielectric in which the workpiece is completely dipped,

$$T_i = T_0 \quad at\ t = 0 \quad (4)$$

Galerkin's finite element method has been applied to obtain temperature distribution within the rectangular domain due to the cylindrical domain and the spark heat flux. The finite element equations can be expressed in matrix form as

$$\left[K_1^{(e)}\right]\overrightarrow{T}^{(e)} + \left[K_2^{(e)}\right]\overrightarrow{T}^{(e)} + \left[K_3^{(e)}\right]\overrightarrow{T}^{(e)} = \overrightarrow{P}^{(e)} \quad (5)$$

where $\left[K_1^e\right] = \iiint_{Ve} [B]^T[D][B]rdV$; [B] is the matrix relating shape function derivative with its nodal value; and [D] is the element matrix. $\left[K_2^e\right] = -\iint_S h[N]^T[N]rds$; [N] is the shape function vector,

$$\left[K_3^e\right] = \iiint_{Ve} \rho c[N]^T[N]rdV$$

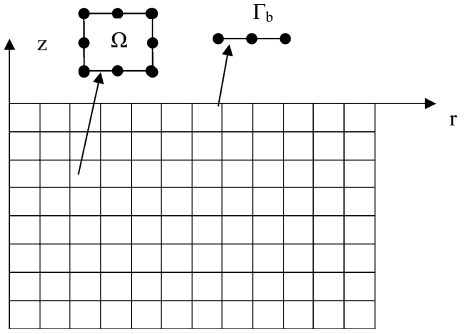


**Fig. 3** Finite element mesh in EDM

$$\overrightarrow{P}^{(e)} = \overrightarrow{P}_2^{(e)} - \overrightarrow{P}_3^{(e)}$$

$$\overrightarrow{P}_2^{(e)} = \iint_S q[N]^T rds\ ;\ \overrightarrow{P}_3^{(e)} = \iint_S hT_0[N]^T rds$$

When the elemental quantities of Eq. 5 are assembled, the following equation is governed

$$KT + M\frac{\partial T}{\partial t} = Q \quad (6)$$

where $K$ is the global conductive matrix; $M$ is the global capacitance; $Q$ is the global heat flux; and $T$ is the global temperature vector.

Implicit finite difference method is used to solve the equation. The following recurrence relation between time steps '0' and '1' is derived

$$(M + \theta\Delta tK)T_1 = [M - (1-\theta)\Delta tK]T_0 + \theta\Delta tQ_1 + (1-\theta)\Delta tQ_0 \quad (7)$$

where $\Delta t$ is time step and $\theta$ is a parameter that can be determined depending on the desired accuracy and stability. The material properties are listed in Table 1. The other conditions are cutting parameters. The cutting parameters are shown in Table 2. The finite element mesh is shown in Fig. 3. The finite element modeling is done with 96 plane rectangular elements. The total nodes are 117. The size of

**Table 2** Cutting parameters

| $\eta$ (%) | $I$ (Amp) | $V$ (Volts) | $R$ (mm) | $q$ (Watts/mm$^2$) | $t_{on}$ (μs) | $t_{off}$ (μs) |
|---|---|---|---|---|---|---|
| 0.40 | 8 | 7 | 0.125 | 4.45 $\eta VI/(\pi R^2)\exp(-4.5(r/R)^2)$ | 8 | 8 |
| 0.40 | 8 | 7 | 0.125 | 4.45 $\eta VI/(\pi R^2)\exp(-4.5(r/R)^2)$ | 10 | 10 |
| 0.40 | 8 | 7 | 0.125 | 4.45 $\eta VI/(\pi R^2)\exp(-4.5(r/R)^2)$ | 12 | 12 |
| 0.40 | 8 | 4 | 0.125 | 4.45 $\eta VI/(\pi R^2)\exp(-4.5(r/R)^2)$ | 8 | 8 |
| 0.40 | 8 | 4 | 0.125 | 4.45 $\eta VI/(\pi R^2)\exp(-4.5(r/R)^2)$ | 10 | 10 |
| 0.40 | 8 | 4 | 0.125 | 4.45 $\eta VI/(\pi R^2)\exp(-4.5(r/R)^2)$ | 12 | 12 |

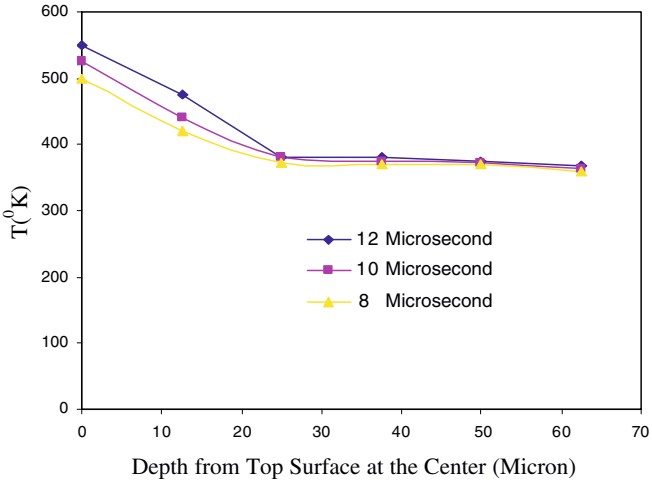


**Fig. 4** Curves of temperature vs. depth from top surface for $V$=7 Volts

elements is 12.5×12.5 μm$^2$. The area shown in Fig. 3 is 150×100 μm$^2$.

## 3 Computational results and validation

### 3.1 Computational results

In this analysis, temperature affected thickness of on-time pulse and discharge voltage on the workpiece surface are examined. Figures 4 and 5 demonstrate how on-time pulse and discharge voltage affect temperature distribution. The maximum temperature near the workpiece surface increases with discharge voltage. The maximum temperatures are 544°K and 439°K for voltage equal to 7 and 4 Volts, respectively. The temperature increases with on-time pulse are shown in Figs. 4 and 5. The thickness of the temperature affected layer determined by a temperature criterion ($T_c$=400°K) is shown in Table 3. The temperature affected layer thickness is determined under the condition

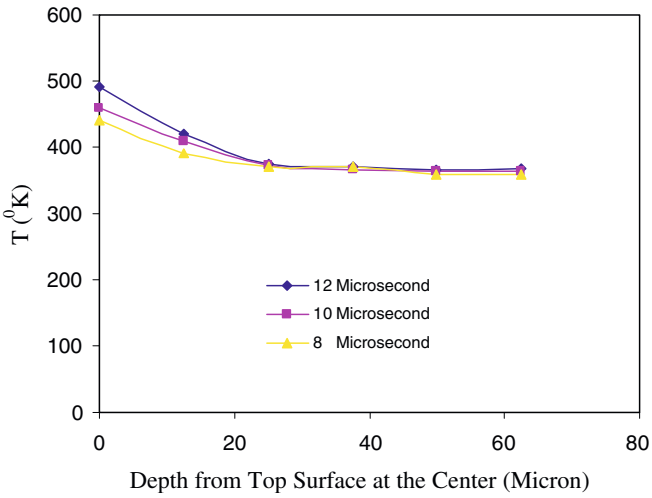


**Fig. 5** Curves of temperature vs. depth from top surface for $V$=4 Volts

**Table 3** Intensively affected layer thicknesses

| On-time pulse (μs) | No load voltage (V) | Temperature affected thickness (μm) |
|---|---|---|
| 8 | 7 | 14.6 |
| 10 | 7 | 18.0 |
| 12 | 7 | 20.9 |
| 8 | 4 | 9.4 |
| 10 | 4 | 13.1 |
| 12 | 4 | 16.9 |

of keeping material thermal properties and some cutting parameters (such as machine cutting speed=1.2 mm/min) constant. In the above simulation, the on-time pulse and discharge voltage are examined. With the change of on-time pulse and discharge voltage, the temperature affected layer thickness has been analyzed. Table 3 shows the minimum thickness is 9.4 μm. The corresponding parameters are $V$=4V and on-time pulse is 8 μs. Then, the smaller the voltage and on-time pulse are, the smaller the temperature affected layer is. On the other hand, machining requires a suitable cutting speed and the corresponding on-time pulse and voltage should be set in order to satisfy both cutting speed and surface integrity requirements.

### 3.2 Experimental validation

In order to investigate the effect of WEDM parameters such as discharge voltage and pulse on-time on the surface damage layer thickness of a machined workpiece, low carbon steel (AISI4340) was used as the cutting material and the varied cutting parameters included discharge duration (on-time) and no load voltage as shown in Table 4.

The other machine factors such as cutting voltage (5V), servo-voltage (10 V), wire tension (1,700 g), wire feed rate (9 m/min), dielectric fluid resistivity (5×10$^4$ Ω.cm), machine speed (1.2 mm/min), and dielectric flushing pressure (8 FR) were kept constant in the investigation. After cutting, the samples were ground and polished so as to enable the surface and sub-surface structures to be observable. The surface damage layer thickness of samples was measured and recorded with a metallography microscope. The data is shown in Table 4. To determine if there is

**Table 4** Affected layer thicknesses of experimental samples

| On time pulse (μs) | No load voltage (V) | Temperature affected thickness (μm) |
|---|---|---|
| 8 | 7 | 15 |
| 10 | 7 | 18.5 |
| 12 | 7 | 20 |
| 8 | 4 | 10.5 |
| 10 | 4 | 12.66 |
| 12 | 4 | 15.75 |

**Table 5** SPSS analysed results for hypothesis testing

| Paired differences | | | | | $t$ |
|---|---|---|---|---|---|
| Mean | Std. deviation | Std. error mean | 95% confidence interval of the difference | | |
| | | | Lower | Upper | |
| .0817 | .884 | .361 | −.846 | 1.009 | .226 |

a difference between computational and tested data, the testing hypotheses are made:

$$H_0 : \mu_c = \mu_t$$
$$H_1 : \mu_c \neq \mu_t$$

Using SPSS software, the analyzed results are shown in Table 5. Since the observed value of the hypothesis testing does not fall in the rejection region ($t$=0.226 is not larger than the upper value 1.009), $H_0$ is accepted. There is sufficient evidence to indicate computational data and testing data are agreeable.

## 4 Conclusions

The optimum cutting parameters of WEDM will reduce temperature affected layer thickness. In the paper, FEM was developed to determine workpiece temperature for different cutting parameters. The thickness of the temperature affected layers for different cutting parameters was computed based on a critical temperature value. Through minimizing the thickness of the temperature affected layers and satisfying a certain cutting speed, a set of the cutting process parameters was determined for workpiece manufacture. A set of optimum parameters for this machining process were selected such that the condition of machine cutting speed was 1.2 mm/min, on time pulse was 8 μs and no load voltage was 4 Volts. The cutting parameters have been validated by the experimental investigation of material manufacture. The analysed results have a good agreement with testing results. Through developing an optimization model to determine cutting parameters by means of FEM, costly and time consuming measurements to determine workpiece temperature affected layers can be reduced. This study is helpful for developing advanced control strategies to enhance the complex contouring capabilities and machining rate while avoiding harmful surface damage.

**Acknowledgements** This research was supported by the National Science Foundation's Engineering Research Center for Reconfigurable Manufacturing Systems. The work is a partnership between the University of Michigan and Morgan State University in advanced manufacturing processes.

## References

1. Wang WM, Rajurkar KP (1992) Modeling and adaptive control of EDM systems. J Manuf Syst 11(5):334–345
2. Ho KH, Newman ST (2003) State of the art electrical discharge machining (EDM). Advanced Manufacturing Systems and Technology Center, Wolfson School of Mechanical and Manufacture Engineering, UK
3. Chou YK, Evans CJ (1999) White layers and thermal modeling of hard turned surfaces. Int J Mach Tools Manuf 39(12): 1863–1881
4. Wojtas AS, Suominen L, Shaw BA, Evans JT (1998) Detection of thermal damage in steel components after grinding using the magnetic Barkhausen noise method. Proceedings of the 7th ECNDT, Copenhagen, 3(9)
5. Velterop L (2003) Influence of wire electrical discharge machining on the fatigue properties of high strength stainless steel. National Aerospace Laboratory NLR, Amsterdam, The Netherlands
6. Blok H (1938) Theoretical study of temperature rise at surfaces of actual contact under oiliness lubricating conditions. Proceedings of general discussion on lubrication and lubricants. Institute of Mechanical Engineers, London, 2:222–235
7. Jaeger JC (1942) Moving sources of heat and the temperature at sliding contacts. J Proc Roy Soc NSW 76:133–228
8. Hahn RS (1951) On the temperature developed at the shear plane in the metal cutting process. Proceedings of the first US national congress of applied mechanics, ASME, pp 661–666
9. Erden A, Kaftanoglu B (1980) Heat transfer modeling of electric discharge machining. Proceeding of the 21st MTDR conference, Swansea, UK, pp 351–358
10. DiBitonto DD, Eubank PT, Patel MR, Barrufet A (1989) Theoretical models of the electrical discharge machining process -I: a simple cathode erosion model. J Appl Phys 66 (9):4104–4111
11. Scott D et al (1991) Analysis and optimization of parameter combination in wire electrical discharge machining process. Int J Prod Res 29(11):2189–2207
12. Biermann D et al (1997) Modeling and simulation of workpiece temperature in grinding by finite element method. Mach Sci Technol 1(2)
13. Bhattacharya R, Jain VK, Ghoshdastidar S (1996) Numerical simulation of thermal erosion in EDM process. J Inst Eng 77:13–19
14. Yadav V, Jain VK, Dixit PM (2002) Thermal stresses due to electrical discharge machining. Int J Mach Tools Manuf 42 (8):887–888
15. Das S, Klotz M, Klocke F (2003) EDM simulation: finite element-based calculation of deformation, microstructure and residual stresses. J Mater Process Technol 142(2):434–451
16. Shi J (2004) Prediction of thermal damage in super finish hard machined surfaces. Dissertation, Purdue University, USA